TRANSPORT PARAMETERS OF MONODISPERSE POROUS CATALYSTS

Pavel Fott[a], Guido Petrini[b] and Petr Schneider[a]

[a] *Institute of Chemical Process Fundamentals, Czechoslovak Academy of Sciences, 165 02 Prague 6 - Suchdol and*
[b] *Istituto Guido Donegani, 281 00 Novara, Italy*

Received October 20th, 1981

A method has been developed of evaluating the transport parameters of porous catalysts using the mean transport pore model (MTPM). The method has been based on combining results of permeation and diffusion measurements while taking into account the different reliability of results of both methods. The approach has been applied to six catalysts for the conversion of water gas with monodisperse pore distribution. Various simple gases have been used to test the MTPM, *i.e.* the independence of transport parameters on experimental conditions. The results have pointed at the shortcomings of estimating the mass transport in porous structures using pore distribution determined by conventional methods.

In some processes in gas–solid systems involving the porous structure of the solids (*e.g.* heterogeneously catalyzed reactions, adsorption, gas–solid reactions, *etc.*) gradients of composition and/or pressure may appear within the porous structure. These gradients give rise to the diffusional and/or permeation mass transfer which may substantially affect the kinetics of the process. For the assessment and prediction of this transport pore distribution curves are being utilized, obtained by mercury porosimetry, eventually in combination with low-temperature physical adsorption (nitrogen, argon, krypton). It turns out quite often (refs[1–5]), however, that these methods do not provide a true picture of the shape and distribution of the pores. For this reason, therefore, the transport of gases in porous media has been characterized by means of effective diffusion coefficients; the measurements being usually carried out with a binary gas mixture at laboratory conditions. These effective diffusion coefficients are suitable, for instance, for comparison of similar porous substances (catalysts, adsorbents *etc.*) but they are ill-suited for predicting the transport properties under different condition (temperature, pressure and composition of multicomponent mixtures).

It therefore appears more advantageous to start from a reasonable model of the porous medium using experimental data on one or more simple transport processes in order to determine the structure-related parameters of the model that do not depend on the conditions of measurement and the kind of gases used (the so called transport parameters). The choice of the model of the porous medium is not arbitrary. It calls for the knowledge of the relationships describing the course of the examined transport processes. Further, one has to be able to describe the process (usually a more complicated one), the course of which is to be predicted (*e.g.* the effect on the catalytic reaction). It is the latter requirement, in particular, that causes that one can work with only very simple model concepts of the porous structure.

The aim of this work has been to show on a series of porous catalysts with monodisperse distribution curves how one can combine the permeation (mass transport due to the pressure gradient) and diffusion measurements (transport due to the composition gradients) using simple gases and gas pairs in order to *i*) determine the transport parameters of a simple model of the porous structure (the mean transport pore mode), *ii*) to test the adequacy of the model and *iii*) to find the relation of the transport parameters to pore distribution curves obtained in the classical way.

THEORETICAL

In the mean transport pore model it has been assumed that owing to the structural properties of the porous medium the transport of gas does not take place necessarily through all pores of the porous solid (the porosity of the transport pores, ε_t, equals at best the total porosity ε). The pores that participate in the transport have been assumed to be straight equal diameter cylinders of radius r (the radius of the transport pore) inclined to the direction of the transport. This inclination causes extension of the transport path (tortuosity). This extension together with the inequality $\varepsilon_t \leqq \varepsilon$ have been incorporated into the second parameter of the model, ψ. The strict concept of identical transport pores in the MTPM may be relaxed by admitting a distributed character of their size. The parameters of the model then become integral means over the transport-pore distribution which depend, in addition, on the method of averaging. As it will be shown in the following, for instance the mean transport pore radius then is not necessarily in a simple relationship to the mean square of this radius $((r^2\psi)/(r\psi) \neq (r\psi)/(\psi)$ and one must use three transport parameters.

For the purely diffusional transport the MTPM permits diffusion to be considered in the transition region between the Knudsen region and the region of bulk diffusion. For the permeation of gases one can incorporate contributions of the Knudsen flow, the viscous flow and the slip at the pore walls. With the aid of the MTPM one can also formulate relationship for the simultaneous diffusion and the forced flow in multicomponent mixtures. This problem arises, for instance, in the assessment of the role of mass transfer in catalytic reactions in porous catalysts.

Real porous materials do not accurately fulfil the concept of the MTPM; for monodisperse narrow pore distribution catalysts, however, the porous structure approximates the idea of the MTPM (and the more closely the narrower the pore distribution). A bidisperse porous solid, will meet the MTPM provided the transport takes place in the interstices between microparticles supporting the micropores with a low transport resistance. In such a case one may expect the transport process to be adequately described by the MTPM.

It has been found[6] that instead of the transport parameters r and ψ it is more convenient to work with combination $r\psi$ and ψ (eventually also with $r^2\psi$); these parameters display a weaker cross-correlation and retain a physical meaning.

EXPERIMENTAL

Catalysts

A series of six porous catalysts for the conversion of water gas (ZnO, CuO, Al_2O_3) shaped as cylindrical pellets was used: commercial catalysts ICI 52-1 (Imperical Chemical Industries) and CCE C183 (Catalyst Chemicals Europe), and experimental catalysts prepared by Montedison and designated as ME-A, ME-B, ME-C and ME-D. The textural properties of the catalysts are summarized in Table I. From the pore distributions obtained by a combination of mercury porosimetry (Porosimeter Erba Science, Milano) and low temperature adsorption of nitrogen (Sorptomatic 1826 of the same manufacturer) it is apparent that all of them may be classified as monodisperse catalysts with different width of the distribution curve.

10 to 12 pellets were used in the diffusional and the permeation experiments, mounted in cylindrical holes of a metal disc whose thickness equalled the length of the pellets. The pellets were first pressed into a piece of undersized silicon rubber tubing and together with the tubing mounted in the opening of the disc.

The Permeation Measurements

The effective permeability coefficients, B (cm^2/s), defined as the ratio of the gas flux through the pellet (mol/cm^2 s) and the gradient of the total molar concentration (mol/cm^4), were determined in the pressure range between 25 and 190 kPa. The data were obtained at the laboratory temperature in a cell described elsewhere[6] by observing the equalization of a small pressure difference (roughly 1 kPa) between two isolated volumes filled with the investigated gas and separated by the metal disc carrying the catalyst pellets. The measurements were carried out with hydrogen, helium, nitrogen and argon; for these gases one can assume negligible surface transport.

Diffusion Measurements

The diffusion measurements were carried out at the laboratory temperature and pressure in a new type of an isobaric cell for counter-current diffusion of a binary gas mixture[7]. The principle of the method utilizes the Graham law, according to which the diffusion fluxes N_A, N_B of gases A and B (mol/cm^2 s) are related by

$$N_A/N_B = -(M_B/M_A)^{1/2}\,, \qquad (1)$$

where M_A, M_B are molecular weights of the gas A and B. For the net diffusion flux N ($N = N_A + N_B$) we then have

$$N = \alpha_{AB} N_A\,, \qquad (2)$$

where $\alpha_{AB} = 1 - (M_A/M_B)^{1/2}$ is nonzero if the molecular weights of both gases are not the same. The net diffusion flux, N, was determined from the velocity of motion of a soap-film in a glass burette connected by one end to that part of the cell filled with gas A. The other part of the cell, flushed by gas B, was vented to the atmosphere, equally as the other end of the glass burette. The pressure difference between both parts of the cell, separated by the metal disc supporting the catalysts pellets, was raised therefore only to a level required to bring about the motion of the soap film and did not exceed 3 Pa (0·02 Torr).

The measurements were carried out with four gas pairs: H_2—N_2, H_2—Ar, He—N_2, He—Ar.

RESULTS AND DISCUSSION

Permeation

The obtained dependences of the effective permeability coefficients B on pressure, p, are illustrated in Fig. 2. The expression for the dependence $B(p)$ according to the

TABLE I
Textural properties of catalysts

Catalyst	S m^2/g	ϱ g/cm^3	ϱ_p g/cm^3	V_p cm^3/g	ε %	Mean pore radius nm	
						a	*b*
ME–B (5 × 5)[c]	85·9	5·03	1·50	0·468	70·2	10·9	9·7
ICI (3·6 × 5)[c]	98·4	4·46	1·53	0·329	65·7	8·7	23·0
ME–C (5 × 5)[c]	76·8	5·03	1·55	0·446	69·2	11·6	11·7
ME–D (5 × 5)[c]	128	4·25	1·54	0·414	63·9	6·5	10·7
ME–A (5 × 5)[c]	83·5	5·03	1·29	0·576	74·4	13·8	20·4
CCE (3·1 × 6·5)[c]	79·9	4·79	1·90	0·318	60·3	8·0	18·3

[a] $2\,V_p/S$; [b] $\langle r \rangle$ Integral mean value from pore distribution; [c] height × diameter of cylindrical pellet (mm).

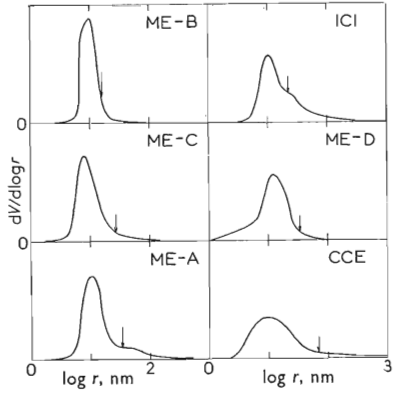

FIG. 1
Pore distribution curves. Arrows indicate the radii of transport pores $(r\psi)_{perm}/(\psi)_{comb}$

MTPM may be obtained easily from the Weber equation[8-10] for the permeability coefficient of a cylindrical capillary in the form

$$B = (r\psi)\,\mathscr{D}^{k*}\,\frac{\omega + (\lambda/2r)}{1 + (\lambda/2r)} + (r^2\psi)\,(p/8\mu)\,, \qquad (3)$$

where $B = N/(-\mathrm{d}c/\mathrm{d}x)$ and N (mol/cm^2 s) is the molar flux of gas of viscosity μ and molecular weight M at pressure p through the porous pellet due to the gradient of the total molar concentration c; $\lambda\ (\sim 1/p)$ is the mean free path of the gas molecules, r is the radius of transport pores and ψ is the geometrical parameter of the porous medium. $\mathscr{D}^{k*} = (2/3)(8RT/\pi M)^{1/2}$ is the Knudsen diffusion coefficient in a capillary of unit radius ($\mathscr{D}^{k}(r) = r\mathscr{D}^{k*}$) and ω is a numerical coefficient, which for a capillary equals[8,9] $\omega = 3\pi/16$ (= 0·589), or[10] $\omega = \pi/4$(= 0·785). The second term on the right hand side of Eq. (3) characterizes the contribution of the viscous (Poiseuille) flow, the first term is the sum of contributions of the Knudsen flow $[(\psi r)\,\mathscr{D}^{k*}(\lambda/2r)/(1 + (\lambda/2r))]$ and the slip at the wall $[(\psi r)\,\mathscr{D}^{k*}\omega/(1 + (\lambda/2r))]$.

Provided $\omega < 0{\cdot}93$, Eq. (3) predicts a minimum on the dependence of B *versus* p. For a porous solid such a minimum has not been unambiguously proved (but see refs[11,12]). Frequent is the case when B at lower pressures depends little on pressure but more strongly so at elevated pressures. Most authors report a linear relationship $B(p)$ which follows from Eq. (3) for $\omega = 1$.

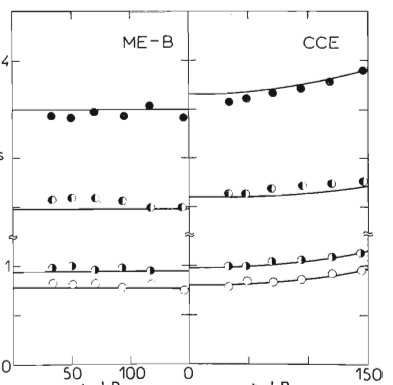

FIG. 2

Pressure dependence of the effective permeability coefficients. Curves computed from Eq. (3) ($\omega = 0{\cdot}9$, $(r\psi)_{perm}$, $(r^2\psi)_{perm}$). ● — H_2, ◐ — He, ◑ — N_2, ○ — Ar

Using $p\lambda/\mu = (\pi/4)(8RT/\pi M)^{1/2}$ from the kinetic theory of gases, one can express Eq. (3) alternatively in the form

$$B/\mathscr{D}^{k*} = (r\psi)\frac{\omega + (\lambda/2r)}{1 + (\lambda/2r)} + (r^2\psi)(3\pi/64)(1/\lambda), \qquad (4)$$

enabling the permeability of different gases in the same porous solid to be described by a single correlation in the coordinate $B/\mathscr{D}^{k*}$ *versus* $(1/\lambda)$ (while $1/\lambda \sim p$).

The effective permeability coefficients of the studied catalysts are plotted in these coordinates in Fig. 3 (the used mean free paths under the atmospheric pressure and the laboratory temperature are summarized in Table II). It is apparent that within the experimental error the experimental points for different gases obey the same dependence and hence confirm the applicability of Eqs (3) and (4).

Eqs (3) and (4) contain three parameters: r, ψ and ω. The transport parameters of the MTPM (r, ψ) were obtained by fitting the experimental data for all gases and a given porous catalyst to Eq. (4) by minimizing the residual sum of squared deviations of $B/\mathscr{D}^{k*}$ for four levels of the parameter ω ($3\pi/16$, $\pi/4$, 0·9 and 1). For all examined catalysts the best agreement between the experimental and the computed

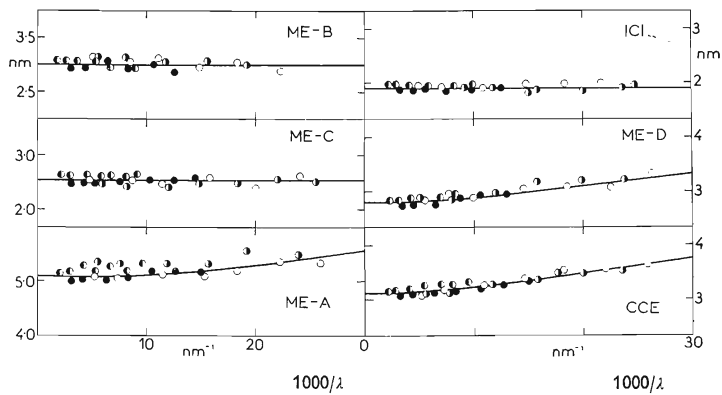

FIG. 3

A plot of $B/\mathscr{D}^{k*}$ *versus* $1/\lambda$. Same symbols as for Fig. 2. Curves computed from Eq. (4). ($\omega = 0{\cdot}9$ and parameters $(r\psi)_{perm}$, $(r^2\psi)_{perm}$)

data was found for $\omega = 0{\cdot}9$. The corresponding optimum parameters of the MTPM are given in Table III in the form $(r\psi)_{perm}$, $(r^2\psi)_{perm}$ together with the confidence limits. The physical meaning of the parameters is apparent from the form of Eq. (*3*) and (*4*). It is seen that for all catalysts the error of determination of the parameter $(r\psi)_{perm}$ is low ($\pm 0{\cdot}05$ nm, *i.e.* 2–3%), while the error of the parameter $(r^2\psi)_{perm}$ is large owing to the minor role of the viscous flow. In view of the inaccuracy of $(r^2\psi)_{perm}$ and possible distribution of the transport pores radii it does not appear advantageous to determine the radius of transport pores as $(r^2\psi)_{perm}/(r\psi)_{perm}$ and the parameter ψ as $(r\psi)^2_{perm}/(r^2\psi)_{perm}$. The good accuracy of the parameter $(r\psi)_{perm}$, however, may be utilized for the determination of ψ from the combination of results of the permeability and diffusion measurements.

TABLE II

Mean free paths[13] λ (101·3 kPa, 298 K) and binary diffusion coefficients[14], $\mathscr{D}^m_{AB}$ (101·3 kPa, 298 K)

Gas	λ, nm	Gas pair	$\mathscr{D}^m_{AB}$, cm^2/s
H_2	123	H_2—N_2	0·776
He	196	H_2—Ar	0·818
N_2	66	He—N_2	0·718
Ar	69	He—Ar	0·748

TABLE III

Transport parameters of catalysts

Catalyst	Permeation measurement		Diffusion measurement		Combined results		
	$(r\psi)_{perm}$ nm	$(r^2\psi)_{perm}$, nm^2	$(r\psi)_{dif}$ nm	$(\psi)_{dif} \cdot 10^2$	$(r\psi)_{perm}$ nm	$(\psi)_{comb} \cdot 10^2$	$(r\psi)_{perm}/(\psi)_{comb}$ nm
ME–B	2·98 ± 0·06	282 ± 75	2·54	8·3	2·98	18·0	16·6
ICI	1·90 ± 0·05	151 ± 62	2·39	4·0	1·90	8·64	22·0
ME–C	2·54 ± 0·04	202 ± 80	4·19	3·3	2·54	9·85	25·8
ME–D	2·81 ± 0·04	163 ± 40	4·52	3·4	2·81	8·29	33·9
ME–A	5·11 ± 0·09	186 ± 109	6·54	8·3	5·11	14·95	34·2
CCE	3·13 ± 0·05	201 ± 56	3·18	4·5	3·13	4·56	68·6

Diffusion

The net fluxes N ($N = N_A + N_B$) for all used pairs A–B (A is the lower molecular weight gas, $M_A < M_B$) and catalysts are given in Table IV.

The molar diffusion flux of the component A in the binary mixture A–B may be described[8,9] with the aid of the MTPM by the differential equation (*5*)

$$N_A = (-c\, \mathrm{d}y_A/\mathrm{d}x)\left[\frac{1 - \alpha_{AB} y_A}{\psi \mathscr{D}^m_{AM}} + \frac{1}{(r\psi)\, \mathscr{D}^{k*}_A}\right]^{-1}, \qquad (5)$$

where y_A (y_B) is the mole fraction of gas A (B) and $r\psi$ and ψ are the transport parameters of the model. The parameter ψ characterizes the contribution of bulk diffusion, the parameter $r\psi$ is decisive for the Knudsen diffusion. The design of the diffusion cell ensures that the tops and the bottoms of the catalyst pellets (length L) are in contact with pure components A and B, *i.e.*

$$\begin{aligned} x = 0 \quad & y_A = 1 \quad & y_B = 0 \\ x = L \quad & y_A = 0 \quad & y_B = 1\,. \end{aligned} \qquad (6)$$

Integration of Eq. (*5*) with the boundary conditions (*6*) and the relationship (*2*) easily yields the expression for the total diffusion flux

$$N = (c/L)\, \mathscr{D}^m_{AB} \ln \frac{(\mathscr{D}^m_{AB}/r\mathscr{D}^{k*}_A) + 1}{(\mathscr{D}^m_{AB}/r\mathscr{D}^{k*}_A) + 1 - \alpha_{AB}}\,. \qquad (7)$$

TABLE IV
Molar diffusion fluxes[a], N (μmol/cm^2 s)

Gas pair	Catalyst					
A–B[b]	ME–B	ICI	ME–C	ME–D	ME–A	CCE
H_2–N_2	1·76	1·51	1·36	1·40	2·68	2·19
H_2—Ar	1·86	1·56	1·52	1·57	2·78	2·27
He—N_2	1·18	0·99	0·92	0·93	1·179	1·43
He—Ar	1·23	1·08	1·02	1·05	1·95	1·59

[a] Length of pellets L — see Table I; [b] gas A in the part of the cell connected to the burette with soap film.

The transport parameters of the model may be determined by direct fitting of the experimentally determined total diffusion fluxes for all gaseous pairs differing by the Knudsen diffusion coefficients $\mathscr{D}_A^{k*}$ and the molecular (bulk) diffusion coefficients $\mathscr{D}_{AB}^{m}$ (see Table II). The fitting is a nonlinear minimization of the sum of squared deviations of the calculated and experimental fluxes N. The shape of Eq. (7), however, enables an alternative procedure: for a given radius r and each pair A–B one can evaluate the argument of the logarithm on the right hand side of Eq. (7). Since the parameter ψ appears in this equation linearly, a linear regression will give an optimum value of ψ to each r as well as the sum of square deviations of computed and measured fluxes N for all pairs on the given catalyst, Q. The thus obtained dependence for the ME–B catalyst in the form of the $(r\psi)$ *versus* ψ plot is shown in figure 4 together with the dependence of Q *versus* $(r\psi)$. The combination of the parameters $(r\psi)_{dif}$ and $(\psi)_{dif}$, corresponding to the minimum of the Q *versus* $(r\psi)$ dependence, is the optimum pair of transport parameters which fits best the experimental diffusion data. These pairs are summarized for all investigated catalysts in Table III. The agreement of the experimental and computed diffusional fluxes N is illustrated in Table IV by average relative deviations; the mean for all catalysts equals 2·2% and the deviation never exceeded 4%.

Owing to the small number of experimental data (4 gaseous pairs) the minimum of the Q *versus* $(r\psi)$ dependence is relatively flat. The 95% confidence limits in the $(r\psi)$ *verus* ψ domain is very narrow in the direction of the axis ψ but it involves the major portion of the curve $(r\psi) - \psi$ forming the bottom-valley line of a three dimensional surface expressing the dependence of the sum of squared deviations, Q, on the parameters $(r\psi)$ and $(Q(r\psi, \psi))$. The pair $(r\psi)_{dif}$, $(\psi)_{dif}$ therefore is not a single combination which fits well the experimental data. Combinations of the values fal-

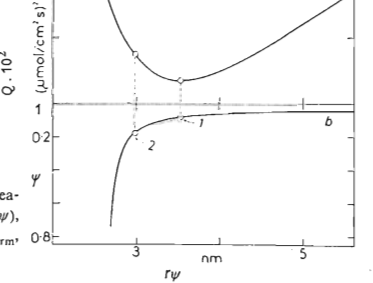

FIG. 4

Dependences obtained from diffusion measurements for catalyst ME–B. *a* Q *versus*$(r\psi)$, *b* ψ *versus*$(r\psi)$ *1* $[(r\psi)_{dif}, (\psi)_{dif}]$, *2* $[(r\psi)_{perm}, (\psi)_{comb}]$

ling onto the bottom-valley line $(r\psi) - \psi$ give an agreement which is statistically only insignificantly worse. It is therefore more correct not to use directly the pairs $(r\psi)_{dif}$, $(\psi)_{dif}$ but to regard as a results of the diffusion measurements the bottom-valley line correlating the optimum parameters $(r\psi) - (\psi)$.

As to the utility of the diffusion equation of MTPM (5) and (7), on can put forth the agreement of the bottom-valley line with the dependences $(r\psi) - \psi$ computed for each gaseous pair separately by solving Eq. (7) (Fig. 5).

Combination of Diffusion and Parmeation Measurements

In view of the good accuracy of the parameter $(r\psi)_{perm}$ obtained from the permeation measurements and the reliability of the bottom-valley line $(r\psi) - \psi$ following from the diffusion measurements it appears reasonable to combine both types of results by obtaining the value $(\psi)_{comb}$ from the bottom-valley line valid for $(r\psi)_{perm}$. The pairs of data obtained in this way are presented in Table III. The prediction of diffusion fluxes utilizing the pairs $(r\psi)_{perm}$, $(\psi)_{comb}$ is only slightly worse then that obtained with pairs $(r\psi)_{dif}$, $(\psi)_{dif}$; from Table V it is apparent that the mean relative deviation of the experimental and computed net diffusion fluxes amounts to 3% and for none of the catalysts exceeds 4%.

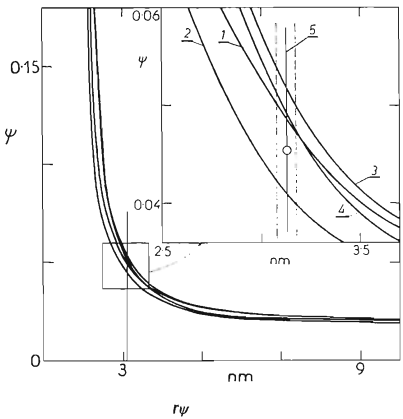

FIG. 5

Dependences ψ *versus*$(r\psi)$ from diffusion measurements with individual gas pairs for the catalysts CCE. *1* H_2—N_2, *2* H_2—Ar, *3* He—N_2, *4* He—Ar, *5* $(r\psi)_{perm}$, ○ — $[(r\psi)_{perm}, (\psi)_{comb}$

From the shape of the bottom-valley line $(r\psi) - \psi$ it is apparent that the accuracy of determination of $(\psi)_{comb}$ stronly depends on the value $(r\psi)_{perm}$. If $(r\psi)_{perm}$ is high then even a considerable error of its value does not cause a significant error of $(\psi)_{comb}$. On the contrary, even a small error in case of a low $(r\psi)_{perm}$ shall cause considerable uncertainty of $(\psi)_{comb}$. This may be demonstrated by expressing the contribution of the resistance of the Knudsen and bulk diffusion from the Bonsanquet formula[15]. The Knudsen diffusion resistance as a a fraction of the total diffusion resistance, K_d, may be expressed as

$$K_d = (r\psi\mathscr{D}_A^{k*})^{-1}/[(r\psi\mathscr{D}_A^{k*})^{-1} + (\psi\mathscr{D}_{AB}^{m})^{-1}] \qquad (8)$$

The error of prediction of the diffusion transport due to relative errors of the parameters $(r\psi)_{perm}$ and $(\psi)_{comb}(\delta(r\psi), \delta(\psi))$ is then proportional to the expression

$$K_d\,\delta(r\psi) + (1 - K_d)\,\delta(\psi)\,. \qquad (9)$$

From Eq. (9) it follows that near the Knudsen region $(K_d \to 1)$ only the error of $(r\psi)$ is of importance. On the contrary, in the proximity of the bulk diffusion region $(K_d \to 0)$ the dominant error is that of the parameter ψ.

In view of the fact that the accuracy of determination of the parameter $(r\psi)_{perm}$ is higher when the contribution of the Knudsen flow to permeation is significant, and *vice versa*, the determination of transport parameters for diffusion has a self-compensating character: more accurate is the parameter of that diffusion mechanism which is more significant. The same selfcomponensation plays a role also in the determination of parameters of the permeation transpoit[6]. On designating the frac-

TABLE V

Relative deviations of computed and experimental diffusion fluxes (%)

Catalyst	With the aid of the parameters	
	$(r\psi)_{dif}$, $(\psi)_{dif}$	$(r\psi)_{perm}$, $(\psi)_{comb}$
ME–B	2·5	2·9
ICI	2·8	3·4
ME–C	1·1	3·0
ME–D	0·5	2·4
ME–A	3·2	3·7
CCE	2·9	3·1

tion of the Knudsen flow and the slip at the pore wall from the net permeation flux as K_p

$$K_p = 1 - [(r^2\psi)(p/8\mu)/B] \qquad (10)$$

the error of prediction of the permeation transport due to the errors of parameters $(r\psi)_{perm}$ and $(r^2\psi)_{perm}$ ($\delta(r\psi)$, $\delta(r^2\psi)$ is proporional to the expression

$$K_p\,\delta(r\psi) + (1 - K_p)\,\delta(r^2\psi)\,. \qquad (11)$$

If, for instance, the contribution of the Knudsen flow and the slip is significant ($K_p \to 1$), the characteristic parameter $(r\psi)_{perm}$ shall be determined more accurately than the parameter of the viscous contribution $(r^2\psi)_{perm}$ and *vice versa* (compare the catalysts ME–B and CCE, Table III, Fig. 2).

Transport Parameters

From the transport parameters $(\psi)_{comb}$, $(r\psi)_{perm}$ and $(r^2\psi)_{perm}$ shown in Table III it follows that the geometry constant $(\psi)_{comb}$ is in all cases relatively low. This may be due to either high tortuosity of the transport pores, or due to the participation of only a small portion of the pores in the transport. If we use in the following considerations for the tortuosity of the transport pores a value of 3 one can conclude that the porosity of the transport pores represents about 43 – 77% of the total porosity with the exception of the catalyst CCE, where it amounts to only 23%. As expected, maximum participation of the pores on the transport (77%) was found for the catalyst ME–B, which in comparison with other catalysts displays the narrowest distribution (Fig. 1). For other catalysts this correlation is not so obvious. Neither is apparent an unambiguous relationship between the radius of the transport pores ($(r\psi)_{perm}/(\psi)_{comb}$; see Table III) and the significant points of the distribution curves, nor the mean pore radii following from the textural data ($\bar{r} = 2V/S$, $\langle r \rangle$; see Table I), even though in all cases the agreement is within an order of magnitude. This is clearly the effect of the simplification and distortion that form an inherent part of evaluation of pore distribution from mercury porosimetry and physical adsorption data.

CONCLUSION

From the performed analysis of diffusion and permeation of simple gases in monodisperse porous solids (catalysts) following conclusions may be drawn: *a*) for prediction and/or characterization of the diffusion behaviour the parameter $(\psi)_{comb}$ and $(r\psi)_{perm}$ are of importance; *b*) the permeation behaviour is characterized by the parameters $(r\psi)_{perm}$ and $(r^2\psi)_{perm}$; *c*) for the description of a combined effect of gradients of composition and pressure the necessary parameters are $(\psi)_{comb}$, $(\psi)_{perm}$, $(r^2\psi)_{perm}$.

LIST OF SYMBOLS

B	effective permeability coefficient
c	total molar concentration
$\mathcal{D}^{k*}$, $\mathcal{D}_A^{k*}$	Knudsen diffusion coefficient in a circular capillary of unit radius
$\mathcal{D}^{k}$	Knudsen diffusion coefficient in a circular capillary
$\mathcal{D}_{AB}^{m}$	bulk diffusion coefficient of pair A–B
K_d	contribution of the Knudsen diffusion resistance to the total resistance
K_p	contribution of the Knudsen flow and slip to the total permeation transport
L	length of the pellet
M, M_A	molecular weight
N, N_A	total molar diffusion flux and diffusion flux of gas A in porous pellet
p	pressure
Q	residual sum of squares
r	pore radius
R	gas constant
S	specific surface
T	temperature
V_p	specific pore volume
x	axial coordinate in pellet
y_A	mole fraction of gas A
α_{AB}	parameter
$\delta(z)$	relative error of quantity z
ε, ε_t	total porosity, porosity of transport pores
λ	mean free path of molecules
μ	gas viscosity
ϱ, ϱ_p	true and apparent density of porous solid
φ	transport parameter
ω	numerical coefficient (slip constant)

REFERENCES

1. Ternan M., Filler O. M.: Can. J. Chem. Eng. *57*, 750 (1979).
2. Ihm S. K., Ruckenstein E.: J. Colloid Interface Sci. *61*, 146 (1977).
3. Scholten J. J. F., Beers A. M., Kiel A. M.: J. Catal. *36*, 23, 30, 36 (1975).
4. Androutsoupoulos G. P., Mann R.: Chem. Eng. Sci. *34*, 1203 (1979).
5. Tomanová D., Zbuzek B., Jeřábek K., Schneider P.: This Journal *46*, 2060 (1981).
6. Fott P., Petrini G.: Appl. Catal. *2*, 367 (1982).
7. Valuš J., Schneider P.: Appl. Catal. *1*, 355 (1981).
8. Schneider P.: Chem. Eng. Sci. *33*, 1311 (1978).
9. Lippert E., Schneider P.: Chem. Eng. Commun. *3*, 65 (1979).
10. Weber S.: Dan. Mat. Fys. Medd. *28* (2), (1954).
11. Grove D. M., Ford M. G.: Nature (London) *182*, 999 (1958).
12. Ash R., Grove D. M.: Trans. Faraday Soc. *453*, 1357 (1960).
13. Hála E.: *Fysikální chemie* II. Academia, Prague 1966.
14. Marrero T. R., Mason E. A.: J. Phys. Chem. Ref. Data *1*, 3 (1972).
15. Pollard W. G., Present R. D.: Phys. Rev. *73*, 762 (1948).

Translated by V. Staněk.